Deletion of rifampicin-inactivating mono-ADP-ribosyl transferase gene of *Mycobacterium smegmatis* globally altered gene expression profile that favoured increase in ROS levels and thereby antibiotic resister generation

Sharmada Swaminath [a,b], Atul Pradhan [a,c], Rashmi Ravindran Nair [a,d], Parthasarathi Ajitkumar [a,*]

[a] *Department of Microbiology and Cell Biology, Indian Institute of Science, Bangalore 560012, Karnataka, India.*
[b] *Department of Biology, University of San Diego, San Diego, CA, USA;*
[c] *Department of Medicine, Renaissance School of Medicine, Stony Brook University, Stony Brook, New York, USA;*
[d] *Department of Microbiology, University of Alabama at Birmingham, Birmingham, Alabama, USA.*

A B S T R A C T

The physiological role of mono-ADP-ribosyl transferase (Arr) of *Mycobacterium smegmatis*, which inactivates rifampicin, remains unclear. An earlier study reported increased expression of *arr* during oxidative stress and DNA damage. This suggested a role for Arr in the oxidative status of the cell and its associated effect on DNA damage. Since reactive oxygen species (ROS) influence oxidative status, we investigated whether Arr affected ROS levels in *M. smegmatis*. Significantly elevated levels of superoxide and hydroxyl radical were found in the mid-log phase (MLP) cultures of the *arr* knockout strain (*arr*-KO) as compared those in the wild-type strain (WT). Complementation of *arr*-KO with expression from genomically integrated *arr* under its native promoter restored the levels of ROS equivalent to that in WT. Due to the inherently high ROS levels in the actively growing *arr*-KO, rifampicin resisters with *rpoB* mutations could be selected at 0 hr of exposure itself against rifampicin, unlike in the WT where the resisters emerged at 12th hr of rifampicin exposure. Microarray analysis of the actively growing cultures of *arr*-KO revealed significantly high levels of expression of genes from succinate dehydrogenase I and NADH dehydrogenase I operons, which would have contributed to the increased superoxide levels. In parallel, expression of specific DNA repair genes was significantly decreased, favouring retention of the mutations inflicted by the ROS. Expression of several metabolic pathway genes also was significantly altered. These observations revealed that Arr was required for maintaining a gene expression profile that would provide optimum levels of ROS and DNA repair system in the actively growing *M. smegmatis*.

1. Introduction

Bacteria of diverse genera are known to inactivate antibiotics through covalent modifications (Davies, 1994; De Pascale and Wright, 2010; Munita and Arias, 2016; Peterson and Kaur, 2018; Egorov et al., 2018). The commonly found covalent modifications are mono-ADP-ribosylation, nucleotidylation, thiol transfer, acylation, phosphorylation, and glycosylation (Egorov et al., 2018). Inactivation of

antibiotics through such covalent modifications forms one of the survival strategies of bacteria in the presence of antibiotics. From bacteria to humans, mono-ADP-ribosylation activity, which is encoded by mono-ADP-ribosyltransferase, is involved in multiple physiological processes (Aravind et al., 2015; Lüscher et al., 2018; Cohen and Chang, 2018). These include DNA damage repair, replication, transcription, cell division, signal transduction, responses to stress and infection, pathogenicity, and aging (Palazzo et al., 2017).

Mycobacterium smegmatis arr gene-encoded product, mono-ADP-ribosyl transferase, inactivates rifampicin through covalent modification (Quan et al., 1999). This gene, which is absent in the pathogenic *Mycobacterium tuberculosis*, is the major contributor to the tolerance of *M. smegmatis* to rifampicin. The presence of *arr* orthologues, in other non-pathogenic and pathogenic bacteria, also confer equally efficient rifampicin-resistance/tolerance (Tanaka et al., 1996; Anderson et al., 1997). An earlier study showed that the catalytic activities of *M. smegmatis* Arr were required to regulate a group of DNA damage responsive genes (Stallings et al., 2011). It also showed that the *M. smegmatis arr* transcription was responsive to DNA damage and oxidative stress and that the non-catalytic part of *M. smegmatis* Arr could bring about the suppression of a set of ribosomal proteins and rRNA as well (Stallings et al., 2011).

Since reactive oxygen species (ROS) cause DNA damage (Cooke et al., 2003; Sakai et al., 2006; Cadet and Wagner, 2014) and Arr was reported to be involved in DNA damage response (Stallings et al., 2011), we suspected a link between Arr and ROS levels. Therefore, in the present study, we compared the levels of hydroxyl radical and superoxide between the MLP cultures of the *arr* knockout strain (*arr*-KO) and the wild-type strain (WT). Since high levels of ROS get generated against

$$\frac{(\ln 2) \times (t_2 - t_1)}{(\ln OD_2 - \ln OD_1)}$$

Or

$$\frac{0.693 \times (t_2 - t_1)}{2.303 \times (\log_{10} OD_2 - \log_{10} OD_1)}$$

some antibiotics in bacteria of diverse genera (Kohanski et al., 2007; Piccaro et al., 2014; Sebastian et al., 2017; Hoeksema et al., 2018; Swaminath et al., 2020), we examined the response of the two strains to rifampicin upon prolonged exposure.

2. Materials and Methods

2.1. Bacterial strains and culture conditions

M. smegmatis (Snapper et al., 1990) wild-type (WT) and *arr* knockout strains (*arr*-KO) (Table S1) were cultured in Middlebrook 7H9 broth (Difco) supplemented with 0.2% glycerol and 0.05% Tween 80 at 37°C, 170 rpm, to mid-log phase (MLP) (OD$_{600\ nm}$ ~0.6). The colony-forming units (CFUs) were determined on Middlebrook 7H10 agar plates. *Staphylococcus aureus* ATCC 25923 (Table S1), which was cultured in Luria-Bertani (LB) broth, was used to determine rifampicin concentration in the culture medium using rifampicin bioassay. *Escherichia coli* JC10289, GM159, and JM109 (Table S1), cultured in LB broth, were used for the propagation of the plasmids used for the generation of *arr*-KO and its complemented strains.

2.2. Generation of M. smegmatis arr knockout mutant (Msm arr-KO)

The knockout mutant (*arr*-KO) of *M. smegmatis arr* (MSMEG_1221) was generated using allelic exchange substrates (AES), as described (van Kessel and Hatfull, 2007), with slight modifications. Standard DNA manipulations were carried out as described (Sambrook and Russell, 2001). The details of the construction of the knockout mutant were given under Supplementary Materials and Methods.

2.3. Construction of arr-KO complemented with genome-integrated Msm arr

Genome integration vector, pMV306 (Stover et al., 1991; Table S1), was used for the integration of *Msm-arr* into *arr*-KO genome for the complementation of *arr*-KO with single copy of *arr* under its own promoter (Table S2 for the primers used). The vector control (pMV306) complemented *arr*-KO also was prepared similarly. The details of these vector constructions were given under Supplementary Materials and Methods.

2.4. Growth characterisation of the M. smegmatis arr-KO and WT

Cultures of the *M. smegmatis* WT and *arr*-KO were started with 1% inoculum in rifampicin-free Middlebrook 7H9 broth that was examined for their OD$_{600\ nm}$ once every 3 hrs using UV-1800 UV-VIS Spectrophotometer (Shimadzu). From the log phase of the respective growth curves of *M. smegmatis* WT and *arr*-KO, the mass doubling time was calculated. Two points from the log phase were selected and the doubling time was calculated as follows (Widdel, 2007):

The OD1 and OD2 correspond to the OD$_{600\ nm}$ values for the corresponding time points, t1 and t2, respectively and ln is natural logarithm.

2.5. Hydroxyl radical and superoxide quantitation using flow cytometry

The levels of hydroxyl radical and superoxide were quantitated in the biological triplicate MLP cultures of WT, *arr*-KO, *arr*-KO/pMV306-*Msm-arr*, and *arr*-KO/pMV306-VC. The samples of each strain were distributed into two tubes labeled, autofluorescence and stained. For hydroxyl radical detection, the cells were stained in the dark at 25°C, with 5 µM (final concentration) (Mukherjee et al., 2009) of 3'-(p-hydroxyphenyl) fluorescein (HPF, Cayman chemicals) (Setsukinai et al., 2003). After incubation at 37°C for 30 min under shaking condition at 170 rpm, the cells were centrifuged and resuspended in Middlebrook 7H9 medium.

For superoxide detection, diethylenetriaminepentaacetic acid (DTPA; 100 µM) was used for preventing redox-active metals mediated reduction of superoxide (Fisher et al., 2004; Yeware et al., 2017). The samples were vortexed to mix with the reagent. A final concentration of 0.5 µM of CellROX Green (Invitrogen), which is a superoxide detecting dye (Choi et al., 2017; McBee et al., 2017), was added to the tube labeled as stained and incubated at 37°C for 120 min under shaking condition at 170 rpm (McBee et al., 2017). The cells were then pelleted down and resuspended in 500 µl of 1x PBS.

The flow cytometry data were collected for 10,000 gated cells using Becton Dickinson FACSVerse flow cytometer with a 488 nm solid-state laser and a 527/32 nm emission filter (GFP) at a low flow rate. While unstained cells were used as the autofluorescence control for hydroxyl radical measurement, the cells with only 10 µM DTPA were used as the autofluorescence control for superoxide analysis. Flow cytometry data

were analysed using FACSuite software. The HPF/CellROX Green median fluorescence of the stained samples was normalised with their respective autofluorescence control. The average normalised HPF/CellROX Green median fluorescence from the three biological replicates was used for plotting the graph. Statistical significance was calculated using a two-tailed paired t-test.

2.6. Hydroxyl radical quantitation using EPR spectrometry

The cells from MLP cultures of WT and *arr*-KO were harvested, snap-frozen in liquid nitrogen, and lysed by mashing with ice-cold Teflon pestle. The lysate in the powdered form was resuspended in 100 mM sodium acetate (200 μl; pH 5.2) and centrifuged at 12000 x g for 5 min at 25°C. The supernatant was mixed with 0.1 M final concentration of 5,5-dimethyl-1-pyrroline N-oxide (DMPO) (Piccaro et al., 2014). Exactly 2 min after DMPO addition, the DMPO-OH adducts were measured. An aqueous flat cell (ES- LC12) was used to load the samples. The EPR analyses were performed in JEOL JES-X3 ESR spectrometer (FA 200), under the parameters: X-band, frequency- 9428.401 (MHz), Power-4.00000 (mW), Field center-337.275(mT), and Sweep time- 2.0 (min). EPR signals were obtained at $g \approx 2$. The Wizard of Baseline and Peaks in Origin® software were used for data processing.

2.7. Determination of Minimum Bactericidal Concentration (MBC) of rifampicin and moxifloxacin for M. smegmatis arr-KO

M. smegmatis arr-KO MLP cultures were exposed to two-fold increasing concentrations of rifampicin (1.5625 μg ml^{-1} to 100 μg ml^{-1}) and moxifloxacin (0.125 μg ml^{-1} to 8 μg ml^{-1}), for a period of 12 hrs, at 170 rpm at 37°C, as described (Swaminath et al., 2020). Subsequently, the cells were mildly sonication using a microprobe at 16% amplitude, 3 pulses of one-second duration each with one-second interval (Vibra Cell, Sonics and Materials Inc., USA), to remove clumps, if any. The samples, before and after the antibiotic exposure, were serially diluted and plated. While plating, care was taken to avoid any antibiotic carryover by washing the cells once with Middlebrook 7H9 broth. The MBC was defined as the lowest concentration of the antibiotic that caused 2-log$_{10}$ units of reduction in the CFU ml^{-1} during the incubation period (Mor et al., 1995).

2.8. Bioassay for rifampicin

The concentration of rifampicin in the liquid cultures was determined using the bioassay with *S. aureus* ATCC 25923 (Table S1), as described (Dickinson et al., 1974), with minor modifications (Sebastian et al., 2017). The details of the bioassay were given under Supplementary Materials and Methods.

2.9. Rifampicin susceptibility of M. smegmatis WT and M. smegmatis arr-KO

The *M. smegmatis* WT and *arr*-KO MLP cultures in biological triplicates were exposed to the respective MBC of rifampicin for 96 hrs. At specific time points, aliquotes of the respective culture were withdrawn, plated on antibiotic-free and rifampicin-containing Middlebrook 7H10 agar, and incubated for 2-3 days at 37°C, to determine the susceptibility and resister generation. The details of the method of rifampicin susceptibility were given under Supplementary Materials and Methods.

2.10. Rifampicin resister generation frequency determination

The resister generation frequency of the rifampicin-surviving population of the respective strain was taken as the average of the resister generation frequencies corresponding to all the respective time points of the antibiotic-surviving phase. This time point was from 24 hr to 48 hr for the WT and from 24 hr to 42 hr for the *arr*-KO. The number of

resisters at a specific time point was divided by the total number of cells at that time point.

2.11. Determination of mutations in the rifampicin resisters

The colonies of WT and the *arr*-KO, isolated from the respective ~3x MBC rifampicin plates, were cultured till MLP in Middlebrook 7H9 broth containing the respective 3x MBC rifampicin. Genomic DNA was extracted, using phenol-chloroform method, as described (Swaminath et al., 2020), with minor changes in the cell lysis procedure. The details of the genomic DNA extraction and determination of RRDR mutations by Sanger sequencing were described under Supplementary Materials and Methods.

2.12. Microarray Analysis

Microarray analyses were performed, using total RNA prepared from the MLP cultures of WT and *arr*-KO, as described (Pradhan et al., 2021). The details of the microarray analysis were given under Supplementary Materials and Methods.

3. Results

3.1. Experimental rationale and strategy

To study the physiological role of Arr, we generated *M. smegmatis arr* knockout mutant strain (*arr*-KO), the *arr*-KO containing genome-integrated single copy *arr* (under its own promoter), and the vector control (VC)-complemented *arr*-KO strains. We determined the growth characteristics and mass doubling time of WT and *arr*-KO. Since Arr was found involved in DNA damage response (Stallings et al., 2011) and ROS cause DNA damage (Keyer et al., 1995; Sakai et al., 2006; Cadet and Wagner, 2013; Cadet and Wagner, 2014), we determined the levels of two ROS, superoxide and hydroxyl radical, in the four actively growing strains. We chose to analyse the levels of superoxide and hydroxyl radical since the first ROS produced is superoxide, which gets dismutated to H$_2$O$_2$ (McCord and Fridovich, 1969; González-Flecha and Demple, 1995), which in the presence of Fe (II) in Fenton reaction (Fenton, 1894), generates the DNA-damaging non-specific mutagenic ROS, hydroxyl radical (Cadet and Wagner, 2014). The levels of the two ROS in WT, *arr*-KO, and *arr / VC* complemented strains were measured using flow cytometry of the cells stained with superoxide- and hydroxyl radical -detecting dyes, and using electron paramagnetic resonance (EPR) spectrometry.

For identifying the molecular basis for the difference between *arr*-KO and WT, RNA from the MLP cultures of the two strains were analysed using microarray. The expression levels were specifically compared for the genes for aerobic respiration, antioxidation, and DNA repair, besides for the genes of many pathways. Based on these data, we predicted the probable reason for the higher levels of ROS in *arr*-KO and the possible physiological role of Arr in the actively growing *M. smegmatis*. Since most often ROS generation had been reported upon antibiotc exposure (Kohanski et al., 2007; Piccaro et al., 2014; Sebastian et al., 2017; Hoeksema et al., 2018; Swaminath et al., 2020), we compared the response of *arr*-KO and WT to rifampicin. For this purpose, the MBC of rifampicin for the two strains was determined. Their response to the respective 2x MBC of rifampicin during prolonged exposure was analysed using CFU readout on rifampicin-free and 3x MBC rifampicin-containing plates, and scoring for rifampicin resister generation.

3.2. Construction and growth characterisation of arr-KO

The *arr*-KO strain, wherein the *arr* gene (MSMEG_1221) was replaced with *hyg^r*, was generated by the allelic exchange method, as described (van Kessel and Hatfull, 2007), with minor modifications. The

recombination event was confirmed by PCR using genomic DNA, and two specific primer sets, as described under Supplementary Methods (Fig. 1A, B). The genetic stability of the *arr*-KO mutant was determined by culturing in the absence of hygromycin for 12 generations in Middlebrook 7H9 medium followed by culturing in the presence of hygromycin for another 12 generations. The mass doubling time and growth rate of *arr*-KO and WT were comparable (Fig. 1C-F). Thus, *arr* gene deletion did not affect the overall growth characteristics of the *arr*-KO and WT, indicating no apparent physiological stress on *arr*-KO. Subsequently, we generated *arr*-KO complemented with *arr* (under its own promoter; *arr*-KO/pMV306-*Msm-arr*) or with vector control (VC; *arr*-KO/pMV306-VC) through genome integration (Fig. S1). The native promoter of *arr* was used for the optimal expression of Arr protein levels that would be comparable to those in WT.

3.3. Superoxide levels were significantly elevated in arr-KO

The levels of superoxide in *arr*-KO, the *arr*/VC complemented strains of *arr*-KO, and WT were determined using CellROX Green (CRG), which detects the ROS (Choi et al., 2017; McBee et al., 2017). CellROX Green stained MLP cells of the samples showed significantly high levels of CRG fluorescence in *arr*-KO, as compared to WT (Fig. 2A; Fig S2A). The complementation with *arr* restored the levels of CRG fluorescence in *arr*-KO/pMV306-*Msm-arr*, but not in *arr*-KO/pMV306-VC, to the levels in WT. These observations confirmed that significantly high levels of superoxide were generated in the absence of *arr* and the complementation of expression with a single copy of *arr* (as in the WT) restored the levels to normalcy as in WT. The significantly elevated levels of superoxide would potentially generate high levels of hydroxyl radical in *arr*-KO. Thus, Arr seemed to be primarily required to maintain levels of

superoxide from which the other two ROS (H_2O_2 and hydroxyl radical) could get generated.

3.4. Significantly high levels of hydroxyl radical in arr-KO

The hydroxyl radical levels were determined using flow cytometry of the intact live cells stained with the hydroxyl radical detecting dye, HPF (Setsukinai et al., 2003). The HPF fluorescence of the MLP cells of *arr*-KO was significantly higher than that of WT MLP cells (Fig. 2B; Fig. S2B). The HPF fluorescence was significantly restored to levels comparable to that in the WT upon complementation with *arr* (*arr*-KO/pMV306-*Msm-arr*), but not with the pMV306-VC vector control (Fig. 2B; Fig. S2B). As expected, the HPF fluorescence levels of *arr*-KO/pMV306-VC (vector control) MLP cells were comparable to those of *arr*-KO MLP cells (Fig. 2B; Fig. S2B). Thus, due to the high levels of superoxide in *arr*-KO, significantly high levels of hydroxyl radical were also formed, favouring mutagenesis of the genome.

However, HPF can detect not only hydroxyl radical but peroxynitrite also (Setsukinai et al., 2003). Peroxynitrite is formed from superoxide and nitric oxide (Koppenol et al., 1992). Since *M. smegmatis* possesses a potential nitric oxide synthase gene (MSMEG_4178), it is possible that the *M. smegmatis* cells might contain peroxynitrite, which in turn could oxidise HPF and elicit fluorescence. Therefore, we wanted to verify the exclusive presence of hydroxyl radical in *arr*-KO and WT cells using electron paramagnetic resonance (EPR) spectrometry, as performed for hydroxyl radical quantitation in the rifampicin exposed *Mtb* cells (Piccaro et al., 2014). The EPR analysis of *arr*-KO and WT MLP cells showed the characteristic strong signal specific to 5,5-dimethyl-1-pyrroline N-oxide (DMPO)-OH adduct indicating elevated levels of hydroxyl radical (Fig. 2C; Fig. S3). The EPR data confirmed the generation of
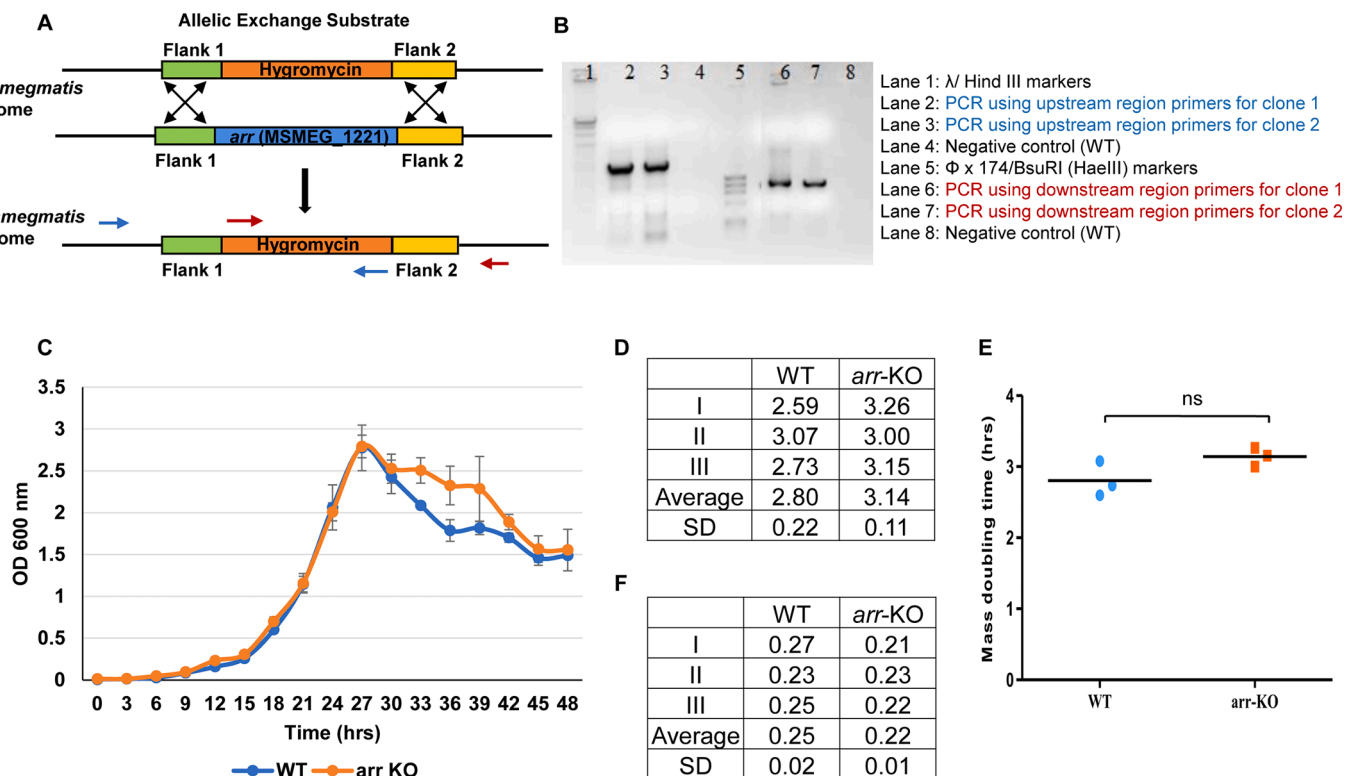
Fig. 1. Generation of *M. smegmatis arr*-KO and comparison of growth characteristics of WT and *arr*-KO. **(A)** Diagrammatic representation of the homologous recombination of allelic exchange substrate used for the generation of *arr*-KO. **(B)** Confirmation of the recombination event by PCR using primers upstream (blue primers in Fig. 1A) and downstream (red primers in Fig. 1A) of the recombination locus. **(C)** Growth curves and **(D)** mass doubling time (calculated from growth curves) of WT and *arr*-KO from the respective biological triplicates. **(E)** Comparison of the mass doubling time of the strains. **(F)** Growth rate of WT and *arr*-KO from the respective biological triplicates in Fig. 1C. The unit of growth rate is hr^{-1}. The statistical significance was calculated using two-tailed unpaired t-test. ns, indicates no significance.

Fig. 2. Detection of superoxide and hydroxyl radical in the MLP cells of *M. smegmatis* WT and *arr*-KO using flow cytometry and EPR. **(A, B)** Flow cytometry profiles of MLP cells of *M. smegmatis* WT, *arr*-KO, *arr*-KO/pMV306-*Msm-arr*, and *arr*-KO/pMV306-VC, stained with CellROX Green for superoxide detection and HPF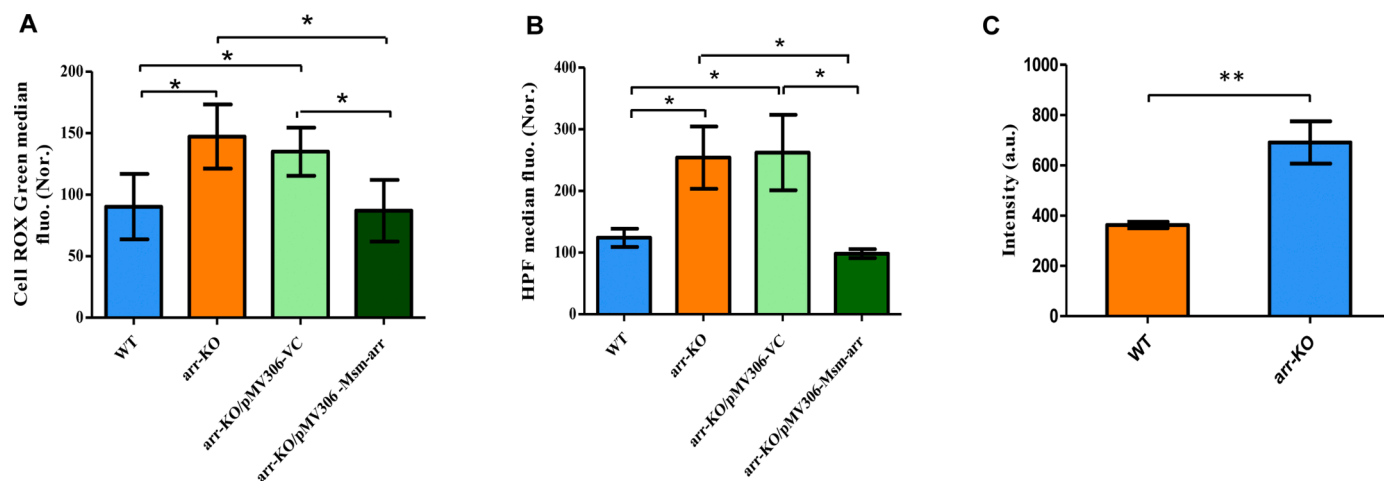 for hydroxyl radical, respectively. **(A)** The average CellROX Green median fluorescence normalised with its respective autofluorescence for the MLP cells of the strains (n = 3). **(B)** The average HPF median fluorescence normalised with its respective autofluorescence for the MLP cells of the strains (n = 3). **(C)** Quantitative levels of DMPO-OH adduct in the MLP cell lysates of the *M. smegmatis arr*-KO and WT (n = 3 biological replicates in each case). One asterisk (*) indicates P ≤ 0.05. The statistical significance was calculated using two-tailed paired t-test.

significantly elevated levels of hydroxyl radical in the absence of Arr. Nevertheless, formation of peroxynitrite could be ruled out as the Middlebrook 7H9 medium does not contain acidified nitrite, which is one of the substrates of nitric oxide synthase to produce nitric oxide (Koppenol et al., 1992). Further, HPF does not either undergo autooxidation to give fluorescence (Setsukinai et al., 2003).

3.5. arr-KO is more susceptible than WT to rifampicin

The absence of Arr, which inactivates rifampicin by covalent modification (Quan et al., 1999), would result in increased sensitivity to rifampicin. We had earlier found 42 μg ml^{-1} to be the 1x MBC rifampicin for 10^8 cells ml^{-1} of WT (Swaminath et al., 2017). But the 1x MBC of rifampicin for 10^8 cells ml^{-1} of *arr*-KO was 2.08 μg ml^{-1}, which was ~20-times lower, indicating its higher rifampicin susceptibility (Fig. S4A, B). However, the 1x MBC for moxifloxacin, which does not get mono-ADP-ribosylated by Arr, was 0.125 μg ml^{-1} for *arr*-KO. It was comparable to 1x MBC moxifloxacin of 0.133 μg ml^{-1} of WT (Fig. S4C, D) (Swaminath et al., 2020). These observations confirmed the specificity of higher rifampicin susceptibility of *arr*-KO and that the target specificity of Arr was confined to rifampicin and not to other antibiotics.

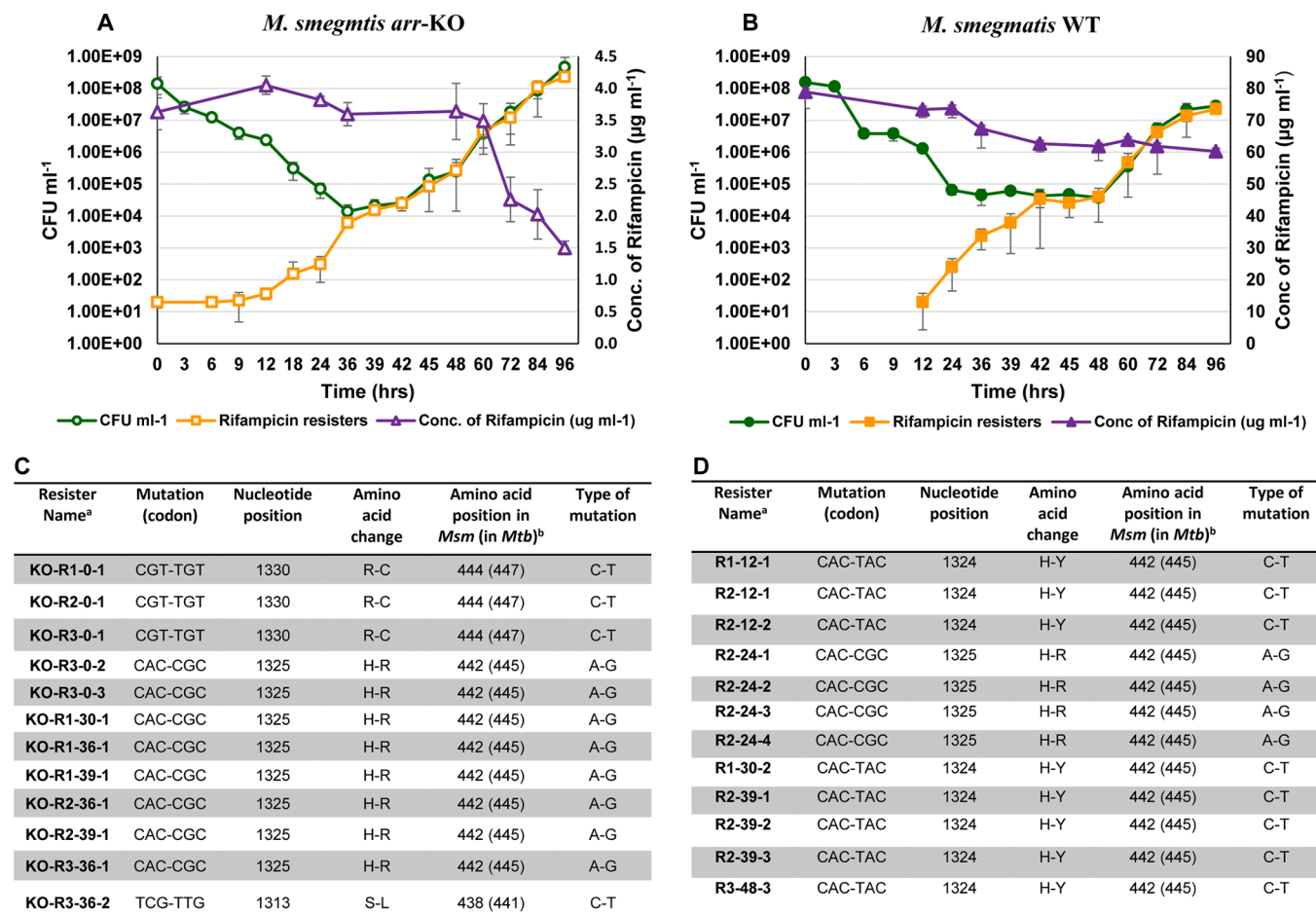### 3.6. Response of arr-KO and WT to rifampicin upon prolonged exposure

3.6.1. The killing, survival, and regrowth of arr-KO and WT

The MLP cultures (10^8 cells ml^{-1}; n = 3 biological replicates in each case) of *arr*-KO and WT were exposed to the respective 2x MBC of rifampicin for 96 hrs to determine the response of the two strains to rifampicin, like our earlier analysis for *M. tuberculosis* and *M. smegmatis* cultures to rifampicin and moxiflixacin, respectively (Sebastian et al., 2017; Swaminath et al., 2020). Aliquots of the cultures were plated at specific intervals on rifampicin-free plates and respective 3x MBC rifampicin-containing plates. The CFU on the rifampicin-free plates showed steady decrease by 3-4 $\log_{10}$ units, followed by more or less no appreciable change, and then a steady increase (Fig. 3A, green line with open green circles, and Fig. 3B, green line with filled green circles, respectively). These indicated a killing phase, survival in the continued presence of rifampicin, and regrowth of the cells from the antibiotic-surviving population. This triphasic response was comparable to those of the *M. smegmatis* and *M. tuberculosis* cultures against moxifloxacin and rifampicin, respectively (Swaminath et al., 2020; Sebastian

et al., 2017). The overall comparability of the triphasic nature of CFU of *arr*-KO and WT against rifampicin indicated that the absence of *arr* might not have altered the response to high MBC of rifampicin. The rifampicin concentration in the *arr*-KO cultures showed only a marginal decrease till 60 hrs, followed by a sudden dip (Fig. 3A, purple line with open purple triangles). Nevertheless, ~1.5 μg ml^{-1} (0.75x MBC) of rifampicin was still present in the *arr*-KO cultures at 96 hr of exposure, despite the sudden decrease at 60 hrs (Fig. 3A, purple line with open purple triangles). On the contrary, the WT cultures showed only a marginal decrease in the rifampicin concentration throughout the period of exposure (Fig. 3B, purple line with filled purple triangles).

3.6.2. Rifampicin resisters of arr-KO could be selected at 0 hr of exposure

From the 0 hr of exposure itself, rifampicin resister colonies emerged from the *arr*-KO cultures (Fig. 3A, orange line with open orange squares). The resister CFU remained without apparent change for the first 9 hrs and then gradually increased till 36 hr. On the contrary, the rifampicin-resisters of WT emerged only from the 12th hr of exposure, followed by a steady increase till 42 hr (Fig. 3B, orange line with filled orange squares). A best fit trend-line of the early steady CFU values of the resisters of *arr*-KO and WT showed that the first rifampicin resister clones emerged at 0 hr and 6 hr, respectively (the dotted blue lines in Fig. S5A and Fig. S5B, respectively). Based on the best fit trend-line, while there were 3 resisters of *arr*-KO at 0 hr, there was only one resister of WT at 6 hr of exposure. On the rifampicin plate, an average (from n = 2) of 20 resister colonies of *arr*-KO could be detected at 0 hr of rifampicin exposure, registering a rifampicin resister generation frequency of 1.391×10^{-7}. On the contrary, there was no resister colony of WT at 0 hr (Fig. S6A, B; Table S3), although plating of the whole cultures of WT, without dilution, would have shown colonies at the natural frequency of 10^{-8} (Swaminath, 2017). Nevertheless, the earlier emergence of larger number of rifampicin resisters from *arr*-KO cultures at 0 hr seemed to have been promoted by the significantly higher levels of ROS formed due to the absence of *arr*. Even at 6 hr of exposure, where the first resister colony of WT was formed, *arr*-KO cultures still showed a higher resister generation frequency of 1.630×10^{-6} as compared to 2.601×10^{-7} of WT cultures (Fig. S6C). However, at 12 hr of rifampicin exposure, where the resister colonies of WT were observed for the first time, the resister generation frequencies of *arr*-KO and WT cultures showed comparable values of 1.564×10^{-5} and 1.477×10^{-5}, respectively (Fig. S6A, B). Thus, over a period of 12 hr of exposure to

A *M. smegmtis arr*-KO

B *M. smegmatis* WT

C

Resister Name[a]	Mutation (codon)	Nucleotide position	Amino acid change	Amino acid position in *Msm* (in *Mtb*)[b]	Type of mutation
KO-R1-0-1	CGT-TGT	1330	R-C	444 (447)	C-T
KO-R2-0-1	CGT-TGT	1330	R-C	444 (447)	C-T
KO-R3-0-1	CGT-TGT	1330	R-C	444 (447)	C-T
KO-R3-0-2	CAC-CGC	1325	H-R	442 (445)	A-G
KO-R3-0-3	CAC-CGC	1325	H-R	442 (445)	A-G
KO-R1-30-1	CAC-CGC	1325	H-R	442 (445)	A-G
KO-R1-36-1	CAC-CGC	1325	H-R	442 (445)	A-G
KO-R1-39-1	CAC-CGC	1325	H-R	442 (445)	A-G
KO-R2-36-1	CAC-CGC	1325	H-R	442 (445)	A-G
KO-R2-39-1	CAC-CGC	1325	H-R	442 (445)	A-G
KO-R3-36-1	CAC-CGC	1325	H-R	442 (445)	A-G
KO-R3-36-2	TCG-TTG	1313	S-L	438 (441)	C-T

D

Resister Name[a]	Mutation (codon)	Nucleotide position	Amino acid change	Amino acid position in *Msm* (in *Mtb*)[b]	Type of mutation
R1-12-1	CAC-TAC	1324	H-Y	442 (445)	C-T
R2-12-1	CAC-TAC	1324	H-Y	442 (445)	C-T
R2-12-2	CAC-TAC	1324	H-Y	442 (445)	C-T
R2-24-1	CAC-CGC	1325	H-R	442 (445)	A-G
R2-24-2	CAC-CGC	1325	H-R	442 (445)	A-G
R2-24-3	CAC-CGC	1325	H-R	442 (445)	A-G
R2-24-4	CAC-CGC	1325	H-R	442 (445)	A-G
R1-30-2	CAC-TAC	1324	H-Y	442 (445)	C-T
R2-39-1	CAC-TAC	1324	H-Y	442 (445)	C-T
R2-39-2	CAC-TAC	1324	H-Y	442 (445)	C-T
R2-39-3	CAC-TAC	1324	H-Y	442 (445)	C-T
R3-48-3	CAC-TAC	1324	H-Y	442 (445)	C-T

[a]Resisters were named in the order of the culture amongst the triplicates, the hour from which they were isolated and the colony number. [b]Amino acid position in *M. tubrculosis* is given in parenthesis. Note: For reporting the amino acid position change in *M. tuberculosis* references *E. coli* numbering is used and 441, 445, 447 amino acid position of *M. tuberculosis* corresponds to 522, 526, 528 of *E. coli*, respectively.

Fig. 3. Rifampicin-susceptibility profile of the *M. smegmatis* MLP cells of *arr*-KO and WT upon prolonged exposure to rifampicin and the emergence of rifampicin resisters. **(A)** Rifampicin susceptibility profile of *arr*-KO exposed to ~2x MBC (4 µg ml^{-1}) of rifampicin for 96 hrs and plated on rifampicin-free plates (green line with open green circle, O), the CFU ml^{-1} on ~3x MBC (6 µg ml^{-1}) rifampicin plates (orange line with open orange square, □) and the concentration of rifampicin during the course of the experiment (right *y*-axis; purple line with open purple triangle, △) (n = 3). **(B)** Rifampicin-susceptibility profile of WT exposed to ~2x MBC (75 µg ml^{-1}) of rifampicin for 96 hrs and plated on rifampicin-free plate (green line with filled green circle, ●), the CFU ml^{-1} on ~3x MBC (125 µg ml^{-1}) rifampicin plates (orange line with filled orange square, ■), and the rifampicin concentration during the experiment (right *y*-axis; purple line with filled purple triangle, ▲) (n = 3). List mutations at the RRDR of *rpoB* of rifampicin resisters of **(C)** *arr*-KO and **(D)** WT.

rifampicin, the rifampicin resister generation frequencies of *arr*-KO and WT became comparable.

3.6.3. Regrowth of the rifampicin surviving populations of arr-KO and WT

The CFU of *arr*-KO and WT on the respective 3x MBC rifampicin plates showed regrowth from the antibiotic-surviving population (Fig. 3A, B, orange line with open and filled orange squares, respectively). The two strains regrew despite the continued presence of ~1.5x MBC rifampicin in the cultures, indicating that the regrowing population would have gained *rpoB* mutations. The CFU scores, from the plates with and without rifampicin, overlapped consistently from the 39 hr and 48 hr of exposure of *arr*-KO and WT cultures, respectively (n = 3 biological replicates in each case). The overlapping showed that the regrowing cells would all have originated from rifampicin-resistant clones, divided using unusual cell division mechanisms and grown, as reported by us recently (Jakkala et al., 2020). Despite both the cultures behaving in a similar manner, the mass doubling time of *arr*-KO from 39 hr onwards was 4.10 hrs and that of WT from 48 hr onwards was 5.25 hrs (Fig. S5C). These differences would have contributed to the final higher cell density

of ~10^9 cells ml^{-1} of *arr*-KO as compared to the ~10^7 cells ml^{-1} of WT at 96 hr (Fig. 3A, B, orange line with open and filled orange squares, respectively).

3.6.4. Rifampicin resistance mutations in the RRDR of arr-KO and WT

Rifampicin resisters would normally contain mutations in the Rifampicin Resistance Determining Region (RRDR) of *rpoB*. Therefore, the RRDR of *rpoB* was sequenced for 12 *arr*-KO resisters obtained from 0 hr (rifampicin unexposed), and from 30 hr, 36 hr, and 39 hr (all from the rifampicin surviving phase). The nucleotide changes were C→T or A→G (Fig. 3C), which were indicative of oxidative stress induced changes (Cadet and Wagner, 2014; Kruetzer and Essigmann, 1998). Similar mutations were detected in the RRDR of 12 rifampicin resisters of WT isolated from the 12 hr (killing phase), 24 hr, 30 hr, 39 hr, and 48 hr (all from the rifampicin surviving phase) (Fig. 3D). The RRDR of *M. tuberculosis* is homologous to the RRDR of *M. smegmatis* at the amino acid level (Fig. S7). Identical nucleotide changes at identical positions had been found in the RRDR of the rifampicin resisters of *M. tuberculosis* from clinical isolates (Telenti et al., 1993; Brandis and Hughes, 2013;

Zaw et al., 2018) and from those that regrew from the rifampicin-surviving population in *in vitro* cultures (Sebastian et al., 2017). The rifampicin-resister generation frequencies of the rifampicin-surviving populations (between the time points indicated as red arrows in Fig. S5A, B and as CFU marked as bold numbers in rows in Table S3) of *arr*-KO and WT (from Fig. 3A, B, respectively) were calculated to be 0.394 ± 0.171 and 0.578 ± 0.2581, respectively. The natural rifampicin resister generation frequency of WT MLP cultures was found to be 10^{-8} by us and another author (Swaminath, 2017; Nyinoh, 2018, respectively). Thus, although the resister generation frequencies of the rifampicin surviving populations of *arr*-KO and WT were different by ~1.5-fold, they were ~8-$\log_{10}$-fold higher than the natural resister generation frquency of their respective MLP cultures. Such high resister generation frequency would be due to exposure to high MBC rifampicin, as reported by us recently (Paul et al., 2022).

3.7. Gene expression profile of arr-KO MLP cells

Since elevated levels of superoxide was observed in the *M. smegmatis arr*-KO actively growing (MLP) cells, leading to high levels of hydroxyl radical and consequential mutagenesis, we performed microarray on the MLP cells of *M. smegmatis arr*-KO and WT, to understand the differential expression of genes between the two strains, caused by the absence of Arr.

3.7.1. High levels of expression of Succinate dehydrogenase I & NADH dehydrogenases

Microarray analysis of the MLP cells of *arr*-KO in comparison to that of WT showed significantly high levels (~1-2-fold) of expression of the aerobic respiration gene NADH-quinone oxidoreductase subunits *CDEGM* (*nuoCDEGM*, MSMEG_2051, MSMEG_2057, 2059, 2060, 2061), which are the NADH interacting subunits of NADH dehydrogenase complex I (Moparthi and Hagerhall, 2011) (Fig. 4A; Supplementary Dataset S1). Other electron transport chain (ETC) genes, including succinate dehydrogenases 1D (*sdh1D*), 1B (*sdh1B*), and A (*sdhA*) belonging to the operon of succinate dehydrogenase I (*sdh1*), also showed ~2-4-fold higher expression (Fig. 4A; Supplementary Dataset S1). In fact, the high levels of Sdh and Nuo have been reported to contribute to superoxide generation by its own autooxidation in *E. coli* (Messner and Imlay, 2002) and mycobacteria (Cook et al., 2014). Surprisingly, the expression levels of the four NADH oxidase genes (*nox*) (MSMEG_1645, MSMEG_2889, MSMEG_2969, MSMEG_6603), which are the other potential superoxide generators in *M. smegmatis* (Fisher et al., 2004; Yeware et al., 2017; Nair et al., 2019), showed but statistically insignificant marginally decreased expression in *arr*-KO (Figure 4B; Supplementary Dataset S1). Therefore, the expression of these genes did not seem to have been affected by the absence of *arr* and are expressed at normal levels in the actively growing *M. smegmatis* (Yeware et al., 2017).

3.7.2. No significant change in the expression of menaquinone biosynthetic genes and genes of crotonase family

Menaquinone/menquinol is the natural conduit between electron-donating and accepting reactions (Cook et al., 2014). Amongst the expression of menaquinone biosynthetic genes (Fig. S8), *menD* and *menB* showed significant reduction by ~1.5-fold and ~2-fold in expression,

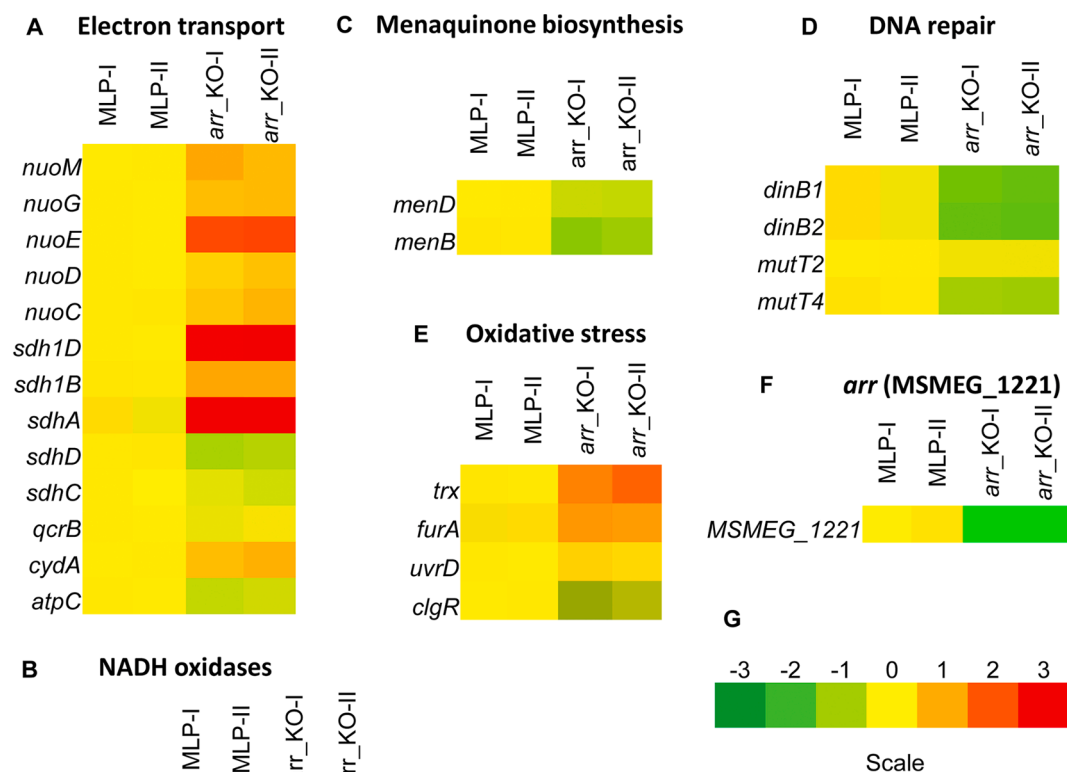**Fig. 4.** Heat Map of *M. smegmatis* MLP cells of WT and *arr*-KO. Heat map of *arr*-KO with respect to WT for: **(A)** electron transport chain genes, **(B)** NADH oxidase genes, **(C)** menaquinone biosynthesis pathway genes, **(D)** DNA repair genes, **(E)** oxidative stress response genes, **(F)** *arr* (MSMEG_1221), at $p < 0.05$, and **(G)** the 3 colour-scale for heat map showing gradients for each fold-change calculated at log base 2.

respectively (Fig. 4C; Supplementary Dataset S1). This decrease in expression of *menD* and *menB* might not have reduced the synthesis of menaquinone, as inhibition of the menaquinone synthesis pathway is lethal to mycobacterial cells (Dhiman et al., 2009). This explanation is supported by the growth kinetics of the *arr*-KO in comparison to WT, which showed comparable growth rate and hence no lethality (see Fig. 1C-F). Thus, in *arr*-KO, while the expression levels of genes of *Sdh1* operon, which normally transfer electrons to menaquinone, were high, there was no corresponding increase in the expression levels of menaquinone biosynthetic genes. Therefore, the elevated levels of electrons, generated by the higher expression of *sdh1b, sdh1D, sdhA* genes, would have got transferred to molecular oxygen, instead of menaquinone, generating significantly high levels of superoxide.

The proteins of the crotonase (or enoyl-CoA hydratase) superfamily catalyse a wide range of metabolic reactions and have a conserved trimeric/ quaternary structure, with a core consisting of (beta/beta/alpha)$_n$ superhelix (Mills et al., 2022). The proteins of this family are usually involved in catalysing dehalogenase, hydratase, and isomerase reactions (Holden et al., 2001). The genes of *M. smegmatis*, besides the menaquinone biosynthetic pathway gene *menB*, belonging to the Crotonase-fold super family, was identified based on their homology with *Mycobacterium tuberculosis* H$_{37}$R$_v$ as well as genes annotated as enoyl CoA hydratase in Mycobrowser (https://mycobrowser.epfl.ch/). In the microarray dataset of *arr*-KO, other than MSMEG_0335, the expression of none of the genes of Crotonase family showed any significant change in comparison to those of WT, indicating that these genes had no contribution to the ROS status of *arr*-KO (Supplementary Dataset S2). Also, the mean change in the expression of MSMEG_0335 of *arr*-KO, which was the only gene that showed statistically significant change (*p* 0.0055), was marginal (~log$_2$ of 0.67) in comparison to that of WT. The functional pathway of this gene has not yet been defined and it lacks functional homology with *M. tuberculosis* H$_{37}$R$_v$.

3.7.3. Low expression levels of DNA repair genes

The expression levels of DNA repair genes were found decreased in the actively growing MLP cells of *arr*-KO (Fig. 4D; Supplementary Dataset S1). Particularly, the levels of expression of *mut*T2 and *mut*T4

genes were significantly low (Fig. 4D; Supplementary Dataset S1). This decrease would support the presence of mutations as early as in the 0 hr of exposure as *mut*T4 has been found to confer tolerance to oxidative stress by preventing misincorporation of 8-oxo-guanine (Dupuy et al., 2020). Thus, the decreased expression of the DNA repair genes facilitated retention of the mutations inflicted by the high levels of hydroxyl radical formed in the absence of *arr*. Among the antioxidant genes, thioredoxin reductase (*trx*, MSMEG_3138), which gets transcriptionally induced upon exposure to oxidative stress (Ritz et al., 2000), and the Fur family transcriptional regulator, *furA* (MSMEG_3460) (Milano et al., 2001), showed significantly increased expression, as would be expected under oxidative stress (Fig. 4E; Supplementary Dataset S1). As an indication of DNA damage in the *arr*-KO cells, there is also a slight but statistically significant increase in the expression of *uvrD* (MSMEG_1941; Supplementary Dataset S1), which is known to get induced upon DNA damage in *E. coli* and *M. tuberculosis* (Siegel, 1983; Chadda et al., 2022, respectively).

3.8. Absence of Arr affects the expression of the genes of several pathways

In addition to the changes in the levels of expression of the genes involved in aerobic respiration, antioxidation, and DNA repair, the absence of Arr caused a global change in the levels of expression of genes participating in several functional categories and pathways (Baloni et al., 2014) and multiple metabolic pathways (Fig. 5A; Supplementary Dataset S3, S4). The different pathways affected (with *p* value < 0.05), as analysed using DAVID database, showed an increased expression of the genes in the ABC transporter and glycerol metabolism pathways, among several other pathways (Fig. 5B; Supplementary Dataset S4). Using DAVID database, we also observed significant levels of decreased expression in the fatty acid degradation and fatty acid metabolism pathways (Fig. 5B; Supplementary Dataset S4). The increased expression of glycerol metabolism genes and decreased expression of fatty acid degradation pathways hinted a metabolic profile indicative of conservation of lipids in *arr*-KO.

Although there was an increase in the expression of ABC transporters, the expression of rifampicin efflux pumps orthologous to those
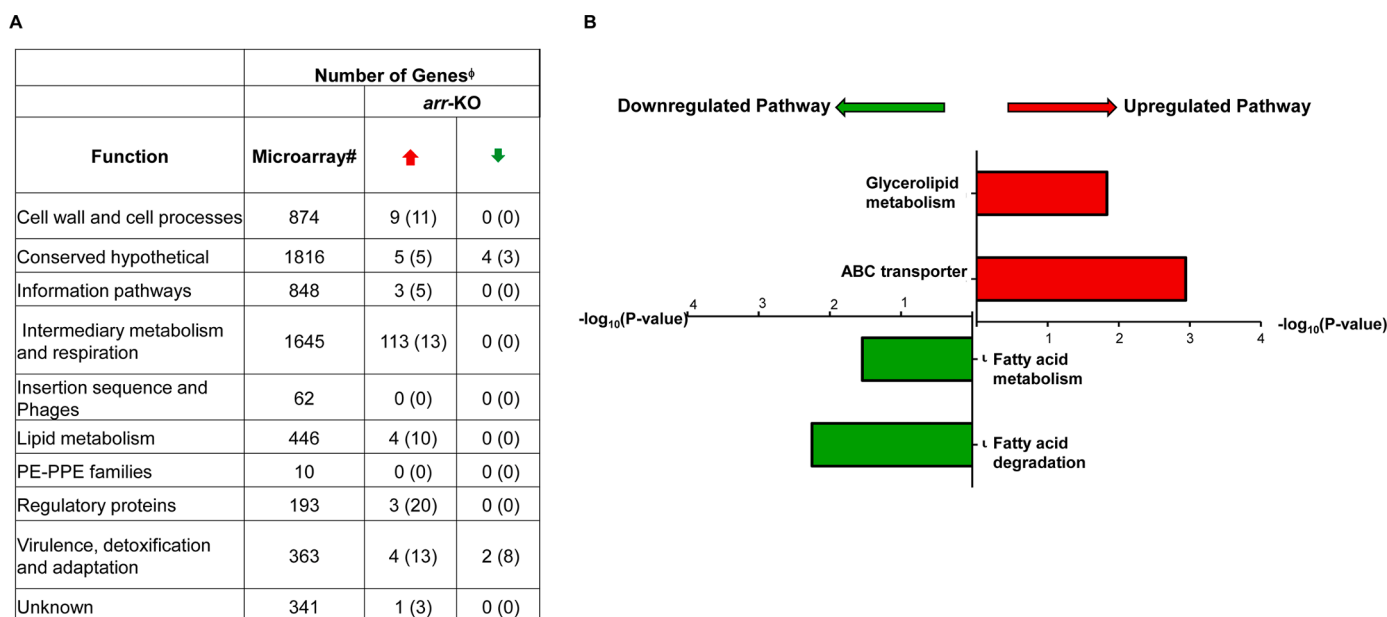
	Number of Genes$^\phi$		
		arr-KO	
Function	**Microarray#**	⬆	⬇
Cell wall and cell processes	874	9 (11)	0 (0)
Conserved hypothetical	1816	5 (5)	4 (3)
Information pathways	848	3 (5)	0 (0)
Intermediary metabolism and respiration	1645	113 (13)	0 (0)
Insertion sequence and Phages	62	0 (0)	0 (0)
Lipid metabolism	446	4 (10)	0 (0)
PE-PPE families	10	0 (0)	0 (0)
Regulatory proteins	193	3 (20)	0 (0)
Virulence, detoxification and adaptation	363	4 (13)	2 (8)
Unknown	341	1 (3)	0 (0)

Fig. 5. Functional categories and pathways of *M. smegmatis arr*-KO with significant differential regulation with respect to WT. **(A)** Summary of the genes of different functional categories showing increased and decreased expression at >2-fold, with significance at *p* < 0.05. The number in the bracket shows the percentage of genes with increased/decreased expression at >2-fold out of the total increased/decreased expression genes with *p* < 0.05, under specific functional categories. Upward red arrow shows increased expression and green downward arrow indicates decreased expression. # All the genes were not present on the array. **(B)** Pathways significantly upregulated and downregulated in *M. smegmatis arr*-KO with respect to WT as analysed by DAVID pathway analysis.

of *M. tuberculosis* $H_{37}R_v$ (Li et al., 2015; Narang et al., 2019) were not increased (Supplementary Dataset S5). It probably indicated that the rifampicin resistance in the *arr*-KO cells were not mediated phenotypically by rifampicin efflux pumps but solely by genetic mutations inflicted by the significantly high levels of hydroxyl radical. The analysis of different pathways, based on the differentially regulated levels of expression of genes in multiple metabolic pathways in the absence of Arr, confirmed that mono ADP ribosylation plays decisive role in the regulation of various metabolic pathways in the actively growing *M. smegmatis*.

4. Discussion

The present study has documented several cellular and molecular changes contributed by the absence of *arr* in the actively growing and rifampicin-exposed *M. smegmatis* cultures. To the best of our knowledge, this is the first time it is shown that the absence of Arr could bring about such conspicuous cellular and molecular changes to the actively growing *M. smegmatis*. It was interesting to note comparable growth parameters despite the absence of *arr* affecting the expression of a multitude of genes in diverse pathways. Through the analysis of the gene expression changes brought about by the absence of Arr, and as hinted by those changes, we attempted to decipher the natural physiological role of Arr in *M. smegmatis*.

4.1. The ROS levels related changes contributed by the absence of arr

The foremost among the changes brought about by the absence of Arr was the inherently higher levels of two ROS, superoxide, and hydroxyl radical, in the actively growing, rifampicin-unexposed *arr*-KO cultures. Since H_2O_2 is formed by the dismutation of superoxide (McCord and Fridovich, 1969; González-Flecha and Demple, 1995), the significantly higher levels of superoxide and hydroxyl radical implied the presence of equivalently higher level of the intermediary ROS, H_2O_2 as well, as shown recently by us in *M. smegmatis* (Paul et al., 2022). From the actively growing *arr*-KO cultures, the selection of rifampicin resisters at a frequency of 1.391×10^{-7}, which is one-$\log_{10}$ higher than the natural mutation frequency (10^{-8}) of *M. smegmatis* against rifampicin (Swaminath, 2017; Nyinoh, 2018), was consistent with the effect of high levels of hydroxyl radical, a DNA-sequence-non-specific mutagen (Keyer et al., 1995; Sakai et al., 2006; Cadet and Wagner, 2013; Cadet and Wagner, 2014). This frequency further increased from 12 hrs of exposure to reach 0.394 ± 0.171 during the rifampicin surviving phase. This drastic increase in the resister generation frequency was due to the high levels of ROS, invoked by the exposure to 2x MBC rifampicin, which overrided and thereby masked the inherently high ROS levels in *arr*-KO. In fact, significantly very high levels of superoxide, H_2O_2, and hydroxyl radical have been found to be present in *M. smegmatis* WT cultures exposed to rifampicin for prolonged duration (Paul et al., 2022). With the slow and steady increase in the ROS levels in the rifampicin exposed WT cultures, the resister generation frequency of WT slowly increased from its natural mutation frequency of 10^{-8} at 0 hr of exposure, to 2.601×10^{-7} at 6 hrs of exposure, which further increased and became comparable to that of *arr*-KO at 12 hr of exposure (1.564×10^{-5} and 1.477×10^{-5}, respectively). Further on, due to the continued exposure to rifampicin, the rifampicin-resister generation frequency increased dramatically to 0.578 ± 0.2581, to become comparable to or even 1.5 times higher than that of *arr*-KO (0.394 ± 0.171). These changes clearly showed that the rifampicin exposure increased ROS levels to all time high despite the absence or presence of Arr.

4.2. The probable gene expression changes contributing to high ROS levels

Since superoxide is the ROS that triggers the sequential formation of H_2O_2 and hydroxyl radical in rifampicin exposed *M. smegmatis* cells (Paul et al., 2022), the significantly higher levels of superoxide in the actively growing *arr*-KO cultures indicated increased expression of superoxide producing genes. In this regard, elevated levels of expression of *Sdh1* genes involved in electron transfer have been found to generate superoxide in *E. coli* (Messner and Imlay, 2002). Succinate dehydrogenase (*sdh1* and *sdh2*) forms complex II of the respiratory chain and couples citric acid cycle, linking an integral part of carbon metabolism with oxidative phosphorylation (Cook et al., 2014). It couples the oxidation of succinate to fumarate in the cytoplasm to the reduction of quinone to quinol in the membrane. The reverse reaction can be catalysed by fumarate reductase, which is generally found in anaerobic or facultative anaerobes (Unden and Bongaerts, 1997). The fumarate reductase under reduced form generates superoxide at high levels when exposed to oxygen in *E. coli* (Imlay, 1995; Messner and Imlay, 2002). In *M. smegmatis*, fumarate reductase is absent (Pecsi et al., 2014), thus prompting *Sdh1* to be the major source of superoxide. Further, Sdh1 can strictly produce superoxide, which can be dismutated to H_2O_2 (Messner and Imlay, 2002), which in turn can undergo Fenton reaction with Fe (II) to generate hydroxyl radical inflicting mutations genome wide. In addition, the NADH-quinone dehydrogenases (*nuoCDEGM*) also would have contributed to superoxide generation.

There was a marginal reduction in the expression of two genes in the menaquinone biosynthetic pathway, *menB* and *menD*. It could be argued that low levels of the electron acceptor menaquinone would have caused electron leak to molecular oxygen promoting superoxide formation. However, the changes in the other five genes (*menACEFG*) in the menaquinone biosynthetic pathway were not statistically significant to bring about a shutdown of the pathway (see the Section c. Menaquinone biosynthesis path in the Supplementary Dataset S1). Further, inhibition of menaquinone biosynthetic pathway in mycobacteria was reported to be lethal (Dhiman et al., 2009). On the contrary, *arr*-KO cells were not suffering from any lethality as the growth characteristics of the *arr*-KO and WT strains were comparable (see Fig. 1C-F). Therefore, the marginal reduction in the expression of *menB* and *menD* would not have affected menaquinone biosynthesis. This probably ruled out the possibility of reduction in the levels of menaquinone that would have otherwise caused electron leak to molecular oxygen.

4.3. The rifampicin-surviving arr-KO cells were not under hypoxia

About 2-3-fold induction of *cydA* and *cydB* in mycobacteria had been reported under low oxygen tension (Kana et al., 2001). In this regard, it could be speculated that the rifampicin surviving *arr*-KO cells might have entered anaerobiosis due to the increased expression of *cydA* (MSMEG_3233; see Section ETC genes *arr*-KO $p < 0.05$ in Supplementary Dataset S1). However, the upregulation of *cydAB* during hypoxia requires the activation of cAMP receptor protein (*cpr1*, MSMEG_6189) (Aung et al., 2014; Ko and Oh, 2020). On the contrary, the expression *cpr1* (MSMEG_6189) in the *arr*-KO MLP population was low (log2 -0.08) in comparison to its expression in the WT (Supplementary Dataset S6). Secondly, the extent of increase in the *cydA* expression was only marginal by $\log_2 0.82$ (~1.7-fold). Thirdly, the genes belonging to *sdh2* (MSMEG_1669 - MSMEG_1672) showed statistically significant reduction in the expression, contrary to their requirement for survival under hypoxic conditions (Pecsi et al., 2014). Fourthly, there was no possibility of hypoxia setting in in the well aerated cultures with 170 rpm shaking. Further, when the cells in the rifampicin surviving population gained *rpoB* mutation, they regrew to establish a rifampicin-resistant population, as reported by us (Jakkala et al., 2020). Thus, taken together, the data suggested very low probability of adaptation of the *arr*-KO cultures to hypoxia under the culture conditions used in the study.

4.4. Involvement of NADH oxidase genes in superoxide production

The four NADH oxidase genes (MSMEG_1645, MSMEG_2889, MSMEG_2969; MSMEG_6603) produce significantly elevated levels of superoxide and hence of hydroxyl radical in the actively growing

M. smegmatis cells (Fisher et al., 2004; Yeware et al., 2017; Nair et al., 2019). However, the expression of these four genes did not show any significant change in the actively growing *arr*-KO (see Fig. 4B; Section b. NADH oxidase *arr*-KO in the Supplementary Dataset S1). Thus, the absence of *arr* did not seem to have caused any change in the expression of the NADH oxidase genes. We did not examine the contribution of NADH oxidase genes to superoxide generation although these genes have been found to generate the ROS in mycobacteria (Nair et al., 2019). Additionally, NADH oxidases have been found to be required for active growth of *M. smegmatis* (Yeware et al., 2017). The absence of any change in the growth rate or mass doubling time of *arr*-KO, as compared to those of WT (see Fig. 1C-F), was consistent with the report (Yeware et al., 2017) as wells as the absence of any significant change in the expression of the NADH oxidase genes.

4.5. The role of Arr in the maintenance of ROS levels in M. smegmatis

The observations in the present study suggested that Arr was required to maintain the levels of expression of specific sets of genes, which included the electron transfer genes that generate superoxide, and thereby hydroxyl radical, in the actively growing *M. smegmatis* cultures. The significant increase in the superoxide and thereby of hydroxyl radical levels in *arr*-KO and their restoration to levels equivalent to those in WT upon complementation of *arr*-KO with *arr* gave the direct evidence for this finding. In view of these observations, it was tempting to speculate that Arr might mono-ADP-ribosylate critical protein factor(s) that might control the expression of electron transfer genes. This in turn would help to maintain superoxide (thereby hydroxyl radical) levels during active growth. The absence of *arr* would disrupt this system thereby enhancing the superoxide/hydroxyl radical levels. This hypothesis would fit well with the increased expression of *Sdh1* genes in *arr*-KO. Besides this possibility, Arr might also directly mono-ADP ribosylate specific components of ETC complexes, thereby activating them for superoxide production. This possibility also gains strength in the light of a report on the mono-ADP-ribosylation of the protein, GcvH-L, by a novel Sirtuin-like protein, SirTM, which resulted in the modulation of oxidative stress response in *Staphylococcus aureus* and *Streptococcus pyogenes* (Rack et al., 2015).

4.6. The global gene expression changes in the absence of Arr

The microarray data showed that besides the increased levels of expression of superoxide producer genes in the actively growing *M. smegmatis arr*-KO cells, the lack of mono-ADP ribosylation by Arr seemed to have significantly affected the expression of several genes involved in diverse metabolic pathways. Based on the global changes found in the *arr*-KO, as reflected by the up/down regulation of many metabolic pathways (see Supplementary Dataset S3,S4), it was reasonable to propose that Arr would be regulating the expression of many genes probably through mono-ADP-ribosylating several gene regulatory proteins that modulate the expression of the genes in these pathways. For example, Arr seemed to have a wide influence on cellular metabolism pathways such as the fatty acid degradation and metabolism (downregulated) and glycerolipid metabolism and ABC transporters (upregulated) (see Fig. 5B; Supplementary Dataset S4). Of course, the modulation of activity of enzymes and other proteins through their direct mon-ADP-ribosylation by Arr is another possibility that was not taken up in the present study.

Mono-ADP ribosylation of diverse substrates by Arr or Arr-like proteins in many organisms have been found to modulate the activity of proteins participating in different physiological functions (Aravind et al., 2015; Palazzo et al., 2017; Cohen and Chang, 2018; Lüscher et al., 2018). Studies to find out the substrates of Arr in *M. smegmatis* showed that Arr mono-ADP-ribosylated 30 kDa and 80 kDa proteins of unknown function (Serres and Ensign, 1996). The BldKB (67 kDa), MalE (45 kDa), and the periplasmic solute binding protein (40 kDa) in *Streptomyces*

coelicolor A3(2) are ADP-ribosylated by the *M. smegmatis arr* orthologue. An extracellular binding protein (~55 kDa), a sugar-binding protein (~45 kDa), and a D-xylose binding periplasmic protein (~40 kDa) of *M. smegmatis* share homology with the three *S. coelicolor* A3(2) proteins, respectively (Letseka, 2010). These observations prompted the speculation that these *M. smegmatis* orthologue proteins may be the substrates of *M. smegmatis* Arr (Letseka, 2010). However, the functional significance of these mono-ADP-ribosylation reactions and the functions of the identified proteins remain to be investigated.

4.7. Differences in the rifampicin response between M. smegmatis arr-KO and the naturally arr-lacking M. tuberculosis

Even though *M. tuberculosis* naturally lacks *arr*, a comparison of the observations from multiple studies reveals conspicuous differences between the response of *M. smegmatis arr*-KO and *M. tuberculosis* to rifampicin. The MBC value of rifampicin for 10^8 cells per ml of *M. smegmatis arr*-KO was 2.08 μg ml^{-1} while it was 0.1 μg ml^{-1} for *M. tuberculosis* cells (Sebastian et al., 2017). Thus, the 20-fold lower MBC of rifampicin for *M. tuberculosis*, indicated a significantly higher susceptibility of *M. tuberculosis* to rifampicin, unlike *arr*-KO, despite the absence of *arr*. The MsRbpA mediated rescue of rifampicin-mediated transcription inhibition and the rifampicin tolerance contributed by *mar*RAB (multiple antibiotic regulators) operon in *M. smegmatis* might have been responsible for the additional tolerance (Tanaka et al., 1996). Secondly, the rifampicin-unexposed *M. smegmatis arr*-KO inherently generated high levels of hydroxyl radical, unlike the rifampicin-unexposed *M. tuberculosis* (Sebastian et al., 2017). Thirdly, rifampicin-resistant *rpoB* mutants emerged from the 0 hr of exposure of *arr*-KO to rifampicin, unlike the emergence of rifampicin-resistant *rpoB* mutants of *M. tuberculosis* from the 10th day of exposure to MBC of the antibiotic (Sebastian et al., 2017). These striking differences between *M. smegmatis arr*-KO and the naturally *arr*-lacking *M. tuberculosis* warrant that their response to rifampicin cannot be compared. Therefore, the proposal to use *M. smegmatis arr* deletion strain as a surrogate system to test anti-tuberculosis drugs, such as rifampicin analogs alone or in combination with other drugs (Agrawal et al., 2015), should be considered with caution.

4.8. Broad significance of the present study

The three-dimensional structure of *M. smegmatis* Arr showed significant homology to eukaryotic mono-ADP-ribosyltransferases and bacterial toxins (Baysarowich et al., 2008). This structural homology implied that the substrates of this enzyme are also quite likely to be similar across the biological systems. Further, mono-ADP-ribosylation has global influence on the metabolism of diverse types of cells (Aravind et al., 2015; Palazzo et al., 2017; Lüscher et al., 2018; Cohen and Chang, 2018), including mycobacteria, as revealed by the microarray analysis in the present study. Further, many species in the *Mycobacterium* genus and of bacteria of diverse genera also possess Arr or Arr-like proteins (Baysarowich et al., 2008). These observations give a broad significance to the present study on the natural physiological role of Arr in *M. smegmatis* as a representative experimental system.

5. Conclusion

M. smegmatis Arr is required for the appropriate expression of specific sets of genes involved in diverse pathways which include genes involved in superoxide production. The regulated expression and/or activity of Arr would have an indirect role on the genesis of antibiotic resisters in bacteria. These specific observations made in the present study are presented in a model (Fig. 6).
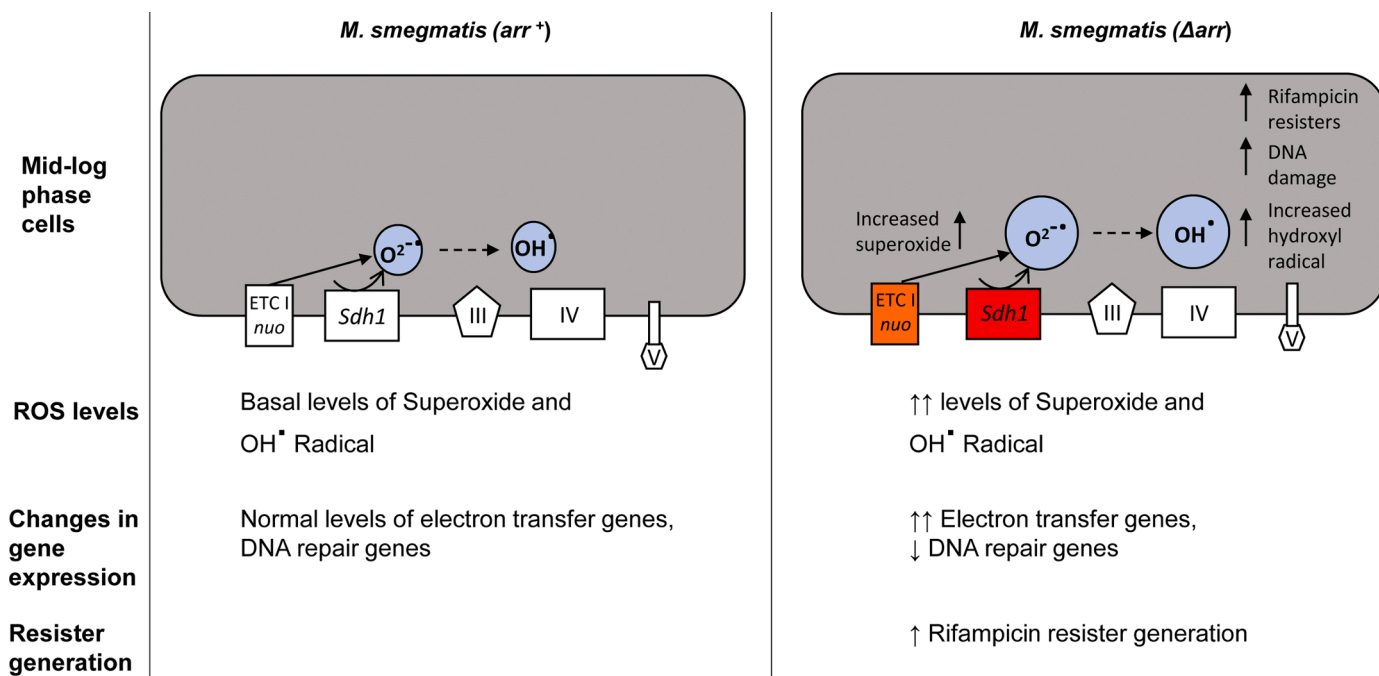
Fig 6. The model presents the specific observations on the increased ROS levels and decreased expression of DNA repair genes favouring generation of mutations. When arr was deleted, it globally altered gene expression profile. Part of this changed expression involved significantly increased expression of electron transfer genes (*sdh1, nuo genes, and probably few others*) and decreased the expression of selected DNA repair genes. This resulted in the increase of the levels of superoxide and hydroxyl radical. The hydroxyl radical inflicted mutations genome wide that could be selected using rifampicin, as rifampicin resisters. The expression of several genes in many other pathways were also either increased or decreased.

Author contributions

PA, SS conceived and designed expts; SS, AP, RRN performed expts; PA, SS, AP, RRN analysed data; PA contributed reagents, materials, and analysis tools; PA, SS wrote the manuscript; all the authors have read and approved the manuscript.

Funding information

Authors thank DBT-IISc Partnership Programme (2012-2020) and Indian Institute of Science for partial funding and DST-FIST, UGC Centre for Advanced Study, ICMR Centre for Advanced Study in Molecular Medical Microbiology and IISc for the infrastructure support. SS, RRN, AP received Senior Research Fellowships from the Council of Scientific and Industrial Research (CSIR), Government of India, and Indian Institute of Science. PA is Emeritus Scientist of the Indian Council of Medical Research (ICMR), Government of India.

Ethical Approval

Not applicable.

CRediT authorship contribution statement

Sharmada Swaminath: Conceptualization, Methodology, Data curation, Writing – original draft. **Atul Pradhan:** Methodology, Data curation, Writing – review & editing. **Rashmi Ravindran Nair:** Methodology, Data curation. **Parthasarathi Ajitkumar:** Conceptualization, Visualization, Investigation, Supervision, Writing – review & editing.

Declaration of Competing Interest

The authors declare that they have no known competing financial interests or personal relationships that could have appeared to influence the work reported in this paper.

Acknowledgements

The present manuscript is an extensively modified version of the article https://doi.org/10.1101/2020.01.10.902668 posted at bioRxiv on 11 January 2020. PA dedicates this work as a tribute to Prof. T. Ramakrishnan (late), who led the pioneering and foundation-laying work on the biochemistry and molecular biology of Mycobacterium tuberculosis at Indian Institute of Science, Bangalore. Authors acknowledge DBT-supported FACS facility, Biological Sciences Division, Indian Institute of Science, and are thankful to Dr. Uttara Chakraborty, Mr. Vasista Adiga, Ms. Urvashi Chauhan, and Ms. Leepika Baid for technical advice and help in flow cytometry measurements.

Supplementary materials

Supplementary material associated with this article can be found, in the online version, at doi:10.1016/j.crmicr.2022.100142.

References

Agrawal, P., Miryala, S., Varshney, U., 2015. Use of Mycobacterium smegmatis deficient in ADP-ribosyltransferase as surrogate for Mycobacterium tuberculosis in drug testing and mutation analysis. PLoS One 10, e0122076. https://doi.org/10.1371/journal.pone.0122076.

Andersen, S.J., Quan, S., Gowan, B., Dabbs, E.R., 1997. Monooxygenase-like sequence of a Rhodococcus equi gene conferring increased resistance to rifampin by inactivating this antibiotic. Antimicrob. Agents Chemother. 41, 218–221. https://doi.org/10.1128/AAC.41.1.218.

Aravind, L., Zhang, D., de Souza, R.F., Anand, S., Iyer, L.M., 2015. The natural history of ADP-ribosyltransferases and the ADP-ribosylation system. Curr. Top. Microbiol. Immunol. 384, 3–32. https://doi.org/10.1007/8_2014_414.

Aung, H.L., Berney, M., Cook, G.M., 2014. Hypoxia-actiavated cytochrome bd expression in Mycobacterium smegmatis is cyclic AMP receptor protein dependent. J. Bacteriol. 196, 3091–3097. https://doi.org/10.1128/JB.01771-14.

Baloni, P., Padiapadu, J., Singh, A., Gupta, K.R., Chandra, N., 2014. Identifying feasible metabolic routes in Mycobacterium smegmatis and possible alterations under diverse nutrient conditions. BMC Microbiology 14, 276. https://doi.org/10.1186/s12866-014-0276-5.

Baysarowich, J., Koteva, K., Hughes, D.W., Ejim, L., Griffiths, E., Zhang, K., Junop, M., Wright, G.D., 2008. Rifamycin antibiotic resistance by ADP-ribosylation: structure

and diversity of Arr. Proc. Natl. Acad. Sci. USA 105, 4886–4891. https://doi.org/10.1073/pnas.0711939105.

Brandis, G., Hughes, D., 2013. Genetic characterisation of compensatory evolution in strains carrying rpoB Ser531Leu, the rifampicin resistance mutation most frequently found clinical isolates. J. Antimicrob. Chemother. 68, 2493–2497. https://doi.org/10.1093/jac/dkt224.

Cadet, J., Wagner, J.R., 2014. Oxidatively generated base damage to cellular DNA by hydroxyl radical and one-electron oxidants: Similarities and differences. Arch. Biochem. Biophys. 557, 47–54. https://doi.org/10.1016/j.abb.2014.05.001.

Chadda, A., Jensen, D., Tomko, E.J., Manzano, A.R., Nguyen, B., Lohman, T.M., Galburt, E.A., 2022. Mycobacterium tuberculosis DNA repair helicase UvrD1 is activated by redox-dependent dimerization via a 2B domain cysteine. Proc. Natl. Acad. Sci. (USA). 119, e2114501119 https://doi.org/10.1073/pnas.2114501119.

Choi, H, Yang, Z, Weisshaar, JC., 2017. Oxidative stress induced in E. coli by the human antimicrobial peptide CM15. PLoS Path 13, e1006481.

Cohen, M.S., Chang, P., 2018. Insights into the biogenesis, function, and regulation of ADP-ribosylation. Nat. Chem. Biol. 14, 236–243. https://doi.org/10.1038/nchembio.2568.

Cook, G.M., Hards, K., Vilcheze, C., Hartman, T., Berney, M., 2014. Energetics of respiration and oxidative phosphorylation in mycobacteria. Microbiol. Spectr. 2 https://doi.org/10.1128/microbiolspec.MGM2-0015-2013, 10.1128/microbiolspec.

Cooke, M.S., Evans, M.D., Dizdaroglu, M., Lunec, J., 2003. Oxidative DNA damage: mechanisms, mutation, and disease. FASEB J 17, 1195–1214. https://doi.org/10.1096/fj.02-0752rev.

Davies, J., 1994. Inactivation of antibiotics and the dissemination of resistance genes. Science 264, 375–382. https://doi.org/10.1126/science.8153624.

De Pascale, G., Wright, G.D., 2010. Antibiotic resistance by enzyme inactivation: from mechanisms to solutions. Chembiochem 11, 1325–1334. https://doi.org/10.1002/cbic.201000067.

Dhiman, R.K., Mahapatra, S., Slayden, R.A., Boyne, M.E., Lenaerts, A., Hinshaw, J.C., Angala, S.K., Chatterjee, D., Biswas, K., Narayanasamy, P., Kurosu, M., Crick, D.C., 2009. Menaquinone synthesis is critical for maintaining mycobacterial viability during exponential growth and recovery from non-replicating persistence. Mol. Microbiol. 72, 85–97. https://doi.org/10.1111/j.1365-2958.2009.06625.x.

Dickinson, J.M., Aber, V.R., Allen, B.W., Ellard, G.A., Mitchison, D.A., 1974. Assay of rifampicin in serum. J. Clin. Path. 27, 457–462. https://doi.org/10.1136/jcp.27.6.457.

Dupuy, P., Howlader, M., Glickman, M.S., 2020. A multilayered repair system protects the mycobacterial chromosome from endogenous and antibiotic-induced oxidative damage. Proc. Natl. Acad. Sci. USA 117, 19517–19527. https://doi.org/10.1073/pnas.2006792117.

Egorov, A.M., Ulyashova, M.M., Rubtsova, M.Yu., 2018. Bacterial enzymes and antibiotic resistance. Acta Naturae 10, 33–48.

Fenton, H.J.H., 1894. LXXIII – Oxidation of Tartaric Acid in presence of Iron. J. Chem. Soc. Trans. 65, 899–910. https://doi.org/10.1039/CT8946500899.

Fisher, A.E.O., Maxwell, S.C., Naughton, D.P., 2004. Superoxide and hydrogen peroxide suppression by metal ions and their EDTA complexes. Biochem. Biophys. Res. Commun. 316, 48–51. https://doi.org/10.1016/j.bbrc.2004.02.013.

González-Flecha, B., Demple, B., 1995. Metabolic sources of hydrogen peroxide in aerobically growing Escherichia coli. J. Biol. Chem. 270, 13681–13687.

Hoeksema, M., Brul, S., Ter Kuile, B.H., 2018. Influence of reactive oxygen species on de novo acquisition of resistance to bactericidal antibiotics. Antimicrob. Agents Chemother. 62, e02354–e023517. https://doi.org/10.1128/AAC.02354-17.

Holden, H.M., Benning, M.M., Haller, T., Gerlt, J.A., 2001. The Crotonase superfamily: divergently related enzymes that catalyze different reactions involving Acyl Coenzyme A Thioesters. Acc. Chem. Res. 34, 145–157.

Imlay, J.A., 1995. A metabolic enzyme that rapidly produces superoxide, fumarate reductase of Escherichia coli. J Biol. Chem. 270, 19767–19777.

Jakkala, K., Paul, A., Pradhan, A., Nair, R.R., Sharan, D., Swaminath, S., Ajitkumar, P., 2020. Unique mode of cell division by the mycobacterial genetic resister clones emerging de novo from the antibiotic-surviving population. mSphere 5, e00994–e009920. https://doi.org/10.1128/mSphere.00994-20.

Kana, B.D., Weinstein, E.A., Avarbock, D., Dawes, S.S., Rubin, H., Mizrahi, V., 2001. Characterization of the cydAB-encoded cytochrome bd oxidase from Mycobacterium smegmatis. J. Bacteriol. 183, 7076–7086. https://doi.org/10.1128/JB.183.24.7076-7086.2001.

Ko, E-M., Oh, J-I., 2020. Induction of the cydAB operon encoding the bd quinol oxidase under respiration-inhibitory conditions by the major cAMP receptor protein MSMEG_6189 in Mycobacterium smegmatis. Front. Microbiol. 11, 608624 https://doi.org/10.3389/fmicb.2020.608624.

Kohanski, M.A., Dwyer, D.J., Hayete, B., Lawrence, C.A., Collins, J.J., 2007. A common mechanism of cellular death induced by bactericidal antibiotics. Cell 130, 797–810. https://doi.org/10.1016/j.cell.2007.06.049.

Koppenol, W.H., Moreno, J.J., Pryor, W.A., Ischiropoulos, H., Beckman, J.S., 1992. Peroxynitrite, a cloaked oxidant formed by nitric oxide and superoxide. Chem. Res. Toxicol. 5, 834–842. https://doi.org/10.1021/tx00030a017.

Kreutzer, D.A., Essigmann, J.M., 1998. Oxidised, deaminated cytosines are a source of C→T transitions in vivo. Proc. Natl. Acad. Sci. USA 95, 3578–3582. https://doi.org/10.1073/pnas.95.7.3578.

Letseka, H.S., 2010. Biochemical characterisation of the Mycobacterium smegmatis rifampicin ADP-ribosylating enzyme Arr [MSc dissertation]. University of Witwatersrand, Johannesburg, South Africa.

Li, G., Zhang, J., Guo, Q., Wei, J., Jiang, Y., Zhao, X., Zhao, L., Lui, Z., Lu, J., Wan, K., 2015. Study of efflux pump gene expression in rifampicin-monoresistant Mycobacterium tuberculosis clinical isolates. J. Antibiot. 68, 431–435. https://doi.org/10.1038/ja.2015.9.

Lüscher, B., Bütepage, M., Eckei, L., Krieg, S., Verheugd, P., Shilton, B.H., 2018. ADP-ribosylation, a multifaceted posttranslational modification involved in the control of cell physiology in health and disease. Chem. Rev. 118, 1092–1136. https://doi.org/10.1021/acs.chemrev.7b00122.

McBee, M.E., Chionh, Y.H., Sharaf, M.L., Ho, P., Cai, M.W.L., Dedon, P.C., 2017. Production of superoxide in bacteria is stress- and cell state-dependent: a gating-optimised flow cytometry method that minimises ROS measurement artifacts with fluorescent dyes. Front Microbiol 8, 459. https://doi.org/10.3389/fmicb.2017.00459.

McCord, J.M., Fridovich, I., 1969. Superoxide dismutase. An enzymic function for erythrocuprein (hemocuprein). J. Biol. Chem. 244, 6049–6055.

Messner, K.R., Imlay, J.A., 2002. Mechanism of superoxide and hydrogen peroxide formation by fumarate reductase, succinate dehygrogenase, and asparatate oxidase. J. Biol. Chem. 277, 42563–42571. https://doi.org/10.1074/jbc.M204958200.

Milano, A., Forti, F., Sala, C., Riccardi, G., Ghisotti, D., 2001. Transcriptional regulation of furA and katG upon oxidative stress in Mycobacterium smegmatis. J. Bacteriol. 183, 6801–6806. https://doi.org/10.1128/JB.183.23.6801-6806.2001.

Mills, C.L., Yin, P., Leifer, B., Ferrins, L., O'Doherty, G.A., Beuning, P.J., Ondrechen, M. J., 2022. Functional Characterization of Structural Genomics Proteins in the Crotonase Superfamily. ACS Chem. Biol. 17, 395–403. https://doi.org/10.1021/acschembio.1c00842.

Moparthi, V.K., Hagerhall, C., 2011. The evolution of respiratory chain complex I from a smaller last common ancestor consisting of 11 protein subunits. J. Mol. Evol. 72, 484–497. https://doi.org/10.1007/s00239-011-9447-2.

Mor, N., Simon, B., Mezo, N., Heifets, L., 1995. Comparison of activities of rifapentine and rifampin against Mycobacterium tuberculosis residing in human macrophages. Antimicrob. Agents Chemother. 39, 2073–2077. https://doi.org/10.1128/AAC.39.9.2073.

Mukherjee, P., Sureka, K., Datta, P., Hossain, T., Barik, S., Das, K.P., Kundu, M., Basu, J., 2009. Novel role of Wag31 in protection of mycobacteria under oxidative stress. Mol. Microbiol. 73, 103–119. https://doi.org/10.1073/pnas.1203735109.

Munita, J.M., Arias, C.A., 2016. Mechanisms of antibiotic resistance. Microbiol. Spectr. 4 https://doi.org/10.1128/microbiolspec.VMBF-0016-2015, 10.1128/microbiolspec.

Nair, R.R., Sharan, D., Ajitkumar, P., 2019. A minor subpopulation of mycobacteria inherently produces high levels of reactive oxygen species that generate antibiotic resisters at high frequency from itself and enhance resister generation from its major kin subpopulation. Front. Microbiol. 10, 1842. https://doi.org/10.3389/fmicb.2019.01842.

Narang, A., Garima, K., Porwal, S., Bhandekar, A., Shrivastava, K., Giri, A., Sharma, N.K., Bose, M., Mandira, V-B., 2019. Potential impact of efflux pump genes in mediating rifampicin resistance in clinical isolates of Mycobacterium tuberculosis from India. PloS One 14, e0223163. https://doi.org/10.1371/journal.pone.0223163.

Nyinoh, I.W., 2018. Spontaneous mutations conferring antibiotic resistance to antitubercular drugs at a range of concentrations in Mycobacterium smegmatis. Drug Dev. Res. 80, 147–154. https://doi.org/10.1002/ddr.21497.

Palazzo, L., Mikoč, A., Ahel, I., 2017. ADP-ribosylation: new facets of an ancient modification. FEBS J 284, 2932–2946. https://doi.org/10.1111/febs.14078.

Paul, A., Nair, R.R., Jakkala, K., Pradhan, A., Ajitkumar, P., 2022. Elevated Levels of Three Reactive Oxygen Species and Fe (II) in the Antibiotic-Surviving Population of Mycobacteria Facilitate De Novo Emergence of Genetic Resisters to Antibiotics. Antimicrob. Agents Chemother. 66, e0228521 https://doi.org/10.1128/aac.02285-21.

Pecsi, I., Hards, K., Ekanayaka, N., Berney, M., Hartman, T., Jacobs Jr, W.R., Cook, G.M., 2014. Essentiality of succinate dehydrogenase in Mycobacterium smegmatis and its role in the generation of membrane potential under hypoxia. mBio 5, e01093–e010914. https://doi.org/10.1128/mBio.01093-14.

Peterson, E., Kaur, P., 2018. Antibiotic resistance mechanisms in bacteria: relationships between resistance determinants of antibiotic producers, environmental bacteria, and clinical pathogens. Front. Microbiol. 9, 2928. https://doi.org/10.3389/fmicb.2018.

Piccaro, G., Pietraforte, D., Giannoni, F., Mustazzolu, A., Fattorini, L., 2014. Rifampin induces hydroxyl radical formation in Mycobacterium tuberculosis. Antimicrob. Agents Chemother. 58, 7527–7533. https://doi.org/10.1128/AAC.03169-14.

Pradhan, A., Swaminath, S., Jakkala, K., Ajitkumar, P., 2021. A method for the enrichment, isolation and validation of Mycobacterium smegmatis population surviving in the presence of bactericidal concentrations of rifampicin and moxifloxacin. FEMS Microbiol. Lett. 368, fnab090. https://doi.org/10.1093/femsle/fnab090.

Quan, S., Imai, T., Mikami, Y., Yazawa, K., Dabbs, E.R., Morisaki, N., Iwasaki, S., Hashimoto, Y., Furihata, K., 1999. ADP-ribosylation as an intermediate step in inactivation of rifampin by a mycobacterial gene. Antimicrob. Agents Chemother. 43, 181–184. https://doi.org/10.1128/AAC.43.1.181.

Rack, J.G.M., Morra, R., Barkauskaite, E., Kraehenbuehl, R., Ariza, A., Qu, Y., Ortmayer, M., Leidecker, O., Cameron, D.R., Matic, I., Peleg, A.Y., Leys, D., Traven, A., Ahel, I., 2015. Identification of a class of protein ADP-Ribosylating Sirtuins in microbial pathogens. Mol. Cell 59, 309–320. https://doi.org/10.1016/j.molcel.2015.06.013.

Ritz, D., Patel, H., Doan, B., Zheng, M., Aslund, F., Storz, G., Beckwith, J., 2000. Thioredoxin 2 is involved in the oxidative stress response in Escherichia coli. J. Biol. Chem. 275, 2505–2512. https://doi.org/10.1074/jbc.275.4.2505.

Sakai, A., Nakanishi, M., Yoshiyama, K., Maki, H., 2006. Impact of reactive oxygen species on spontaneous mutagenesis in Escherichia coli. Genes Cells 11, 767–778. https://doi.org/10.1111/j.1365-2443.2006.00982.x.

Sambrook, J., Russell, D.W., 2001. Molecular Cloning: A Laboratory Manual, 3rd edition. Cold Spring Harbor Laboratory Press, New York, NY.

Sebastian, J., Swaminath, S., Nair, R.R., Jakkala, K., Pradhan, A., Ajitkumar, P., 2017. De novo emergence of genetically resistant mutants of Mycobacterium tuberculosis from the persistence phase cells formed against antituberculosis drugs in vitro. Antimicrob. Agents Chemother. 61, e01343–e013416. https://doi.org/10.1128/AAC.01343-16.

Serres, M.H., Ensign, J.C., 1996. Endogenous ADP-ribosylation of proteins in Mycobacterium smegmatis. J. Bacteriol. 178, 6074–6077. https://doi.org/10.1128/jb.178.20.6074-6077.1996.

Setsukinai, K., Urano, Y., Kakinuma, K., Majima, H.J., Nagano, T., 2003. Development of novel fluorescence probes that can reliably detect reactive oxygen species and distinguish specific species. J. Biol. Chem. 278, 3170–3175. https://doi.org/10.1074/jbc.M209264200.

Siegel, E.C., 1983. The Eschsrichia coli uvrD gene is inducible by DNA damage. Mol. Gen. Genet. 191, 397–400.

Snapper, S.B., Melton, R.E., Mustafa, S., Kieser, T., Jacobs Jr., W.R., 1990. Isolation and characterisation of efficient plasmid transformation mutants of Mycobacterium smegmatis. Mol. Microbiol. 4, 1911-1919. doi: 10.1111/j.1365-2958.1990.tb02040.x.

Stallings, C.L., Chu, L., Li, L.X., Glickman, M.S., 2011. Catalytic and non-catalytic roles for the mono-ADP-ribosyltransferase Arr in the mycobacterial DNA damage response. PLoS One 6, e21807. https://doi.org/10.1371/journal.pone.0021807.

Stover, C.K., de la Cruz, V.F., Fuerst, T.R., Burlein, J.E., Benson, L.A., Bennett, L.T., Bansal, G.P., Young, J.F., Lee, M.H., Hatfull, G.F., Snapper, S.B., Barletta, R.G., Jaconds Jr., W.R., Bloom, B.R., 1991. New use of BCG for recombinant vaccines. Nature 351:456-460. doi: 10.1038/351456a0.

Swaminath, S., 2017. Cellular and Molecular Features of the Response of Mycobacterium smegmatis to Rifampicin and Moxifloxacin upon Prolonged Exposure [PhD thesis]. Indian Institute of Science, Bangalore, India.

Swaminath, S., Paul, A., Pradhan, A., Sebastian, J., Nair, R.R., Ajitkumar, P., 2020. Mycobacterium smegmatis moxifloxacin persister cells produce high levels of hydroxyl radical, generating genetic resisters selectable not only with moxifloxacin, but also with ethambutol and isoniazid. Microbiology 166, 180–198. https://doi.org/10.1099/mic.0.000874.

Tanaka, Y., Yazawa, K., Dabbs, E.R., Nishikawa, K., Komaki, H., Mikami, Y., Miyaji, M., Morisaki, N., Iwasaki, S., 1996. Different rifampicin inactivation mechanisms in Nocardia and related taxa. Microbiol. Immunol. 40, 1–4. https://doi.org/10.1111/j.1348-0421.1996.tb03303.x.

Telenti, A., Imboden, P., Marchesi, F., Lowrie, D., Cole, S., Colston, M.J., Matter, L., Schpfer, K., Bodmer, T., 1993. Detection of rifampicin-resistance mutations in Mycobacterium tuberculosis. Lancet 341, 647–650. https://doi.org/10.1016/0140-6736(93)90417-f.

Unden, G., Bongaerts, J., 1997. Alternative respiratory pathways of Escherichia coli: energetics and transcriptional regulation in response to electron acceptors. Biochim. Biophys. Acta 1320, 217–234. https://doi.org/10.1016/s0005-2728(97)00034-0.

Van Kessel, J.C., Hatfull, G.F., 2007. Recombineering in Mycobacterium tuberculosis. Nat. Methods 4, 147–152. https://doi.org/10.1038/nmeth996.

Widdel, F., 2007. Theory and measurement of bacterial growth. Di Dalam Grundpraktikum Mikrobiologie 4, 1–11.

Yeware, A.M., Shurpali, K.D., Athalye, M.C., Sarkar, D., 2017. Superoxide generation and its involvement in the growth of Mycobacterium smegmatis. Front Microbiol. 8, 105. https://doi.org/10.3389/fmicb.2017.00105.

Zaw, M.T., Emran, N.A., Lin, Z., 2018. Mutations inside rifampicin-resistance determining region of rpoB gene associated with rifampicin-resistance in Mycobacterium tuberculosis. J. Infect. Public Health 11, 605–610. https://doi.org/10.1016/j.jiph.2018.04.005.